

# Flow and motion behavior of particle suspensions in shear flow over a rough surface

V. Mikulich & C. Brücker

*Institute of Mechanics and Fluid Dynamics,  
TU Bergakademie Freiberg, Germany*

## Abstract

The paper discloses the experimental study results of the behavior of a thin layer of low concentrated slurry in a shear flow over a rough surface with a defined structure of the bottom wall. A new ring shear device was built which contains an optically transparent test chamber of which the bottom wall contains arrays of micro-cantilever force sensors simulating a defined surface roughness. It was created by deep-etching of micro-pillars in a silicon wafer. The results of visual observation of the interaction of the suspension with the structured surface during severe deformation are shown. Observation covered the liquid phase motion by micro-PIV, the interaction between the liquid phase and solid particles, the movement of separate particles and their mutual interaction. The contact interactions between particles and micro-pillars are exemplified. The abrupt changes in rotational motion and translational velocity of particles induce mutual collisions and continuous formation and break-up of cluster structures of various types.

*Keywords: slurry, shear flow, micro-structured surface, particle interaction, micro-pillars, cantilever-array, force-measurements.*

## 1 Introduction

In many technical applications of material processing and process technology, such as grinding, lapping, and wire sawing, suspensions of particles and the carrier fluid (slurries) are used to support the micro-mechanical removal and to ensure the transport of the particles. Here, the removal process is usually carried out in a narrow gap between the process tool and the workplace surface. The complex mechanical behavior of particles in interaction with the walls and



multiple contacts with each other in the process gap as well as cluster formation and break-up are not understood sufficiently yet. Experimental study of such systems is very scarce. Hence, detailed analysis of the process parameters with the specific requirement of the surface structures is impossible.

This paper presents a new experimental reference-model for processes in gap flows, which is based on microscopic measurement techniques of the forces at particle-wall interaction as well as the flow behavior at the micro scale. The reference model has defined boundary conditions regarding to the roughness and the fracture behavior of the surface which offers unique possibilities for comparison and validation of the numerical simulations.

## 2 Experimental details

Up to now, measurement of shearing behaviour of slurries has been carried out in different types of ring shear testers as discussed in Bjerrum and Landva [1], Bishop *et al.* [2], Bromhead [3], Carr and Walker [4]. The present study was carried out using a new ring shear device that contains an optically transparent test chamber which allows observing the slurry deformations as well as the particle-wall contact forces (see Fig. 1). In addition, the global parameters such as axial load, torque and gap width can be controlled, too. The instrument's particular feature is the spring-loaded joint between the mobile ring and the loading system so that the ring is able to adapt to changes in the internal slurry forces in axial and torsional directions. Different spring stiffness can be applied in the set-up. The axial spring counteracts the value of axial loads being built up in the shear flow. Such type of loading corresponds with many methods of surface-processing of materials. The torsional spring at the joint of the ring allows watching stick-slip behavior caused by cluster formation and break-up in the suspension.

The narrow test chamber is defined by the outer edges of a glass ring as shown in Fig. 2. The inner and outer diameter of the ring is 90 mm and 110 mm, respectively. The slurry is held in the gap between the upper glass ring and the fixed bottom wall. Shear is imposed by rotation of the upper ring under defined axial load and rotation speed. The bottom wall represents the micro-structured surface we used for the analysis of deformation, damage and wear in industrial silicon processing (see Fig. 3). The surface was created by etching micro-pillars that simulated surface roughness and at the same time were force sensors of the type of micro-cantilever beams according the measurement principle described in Brücker *et al.* [5] and Brücker [6]. The deformation and fracture of the micro-pillars during interaction with the particles in the suspension are detected by imaging from top and the side-walls. Brücker *et al.* [5] and Brücker [6] used such an array of flexible micro-hairs in the form of small slender micro-pillars made from an elastomer to measure the wall friction force distribution in turbulent flows. The same principle is applied herein to measure the contact forces during interaction of the particles with the walls.

The slurry consisted of the mixture of glycerine as the fluid phase and glass balls in diameter 400  $\mu\text{m}$ –750  $\mu\text{m}$ , coated with fluorescent material. For flow



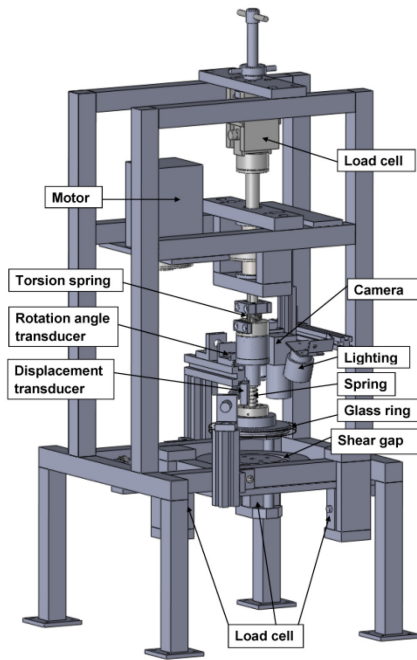


Figure 1: Ring shear apparatus.

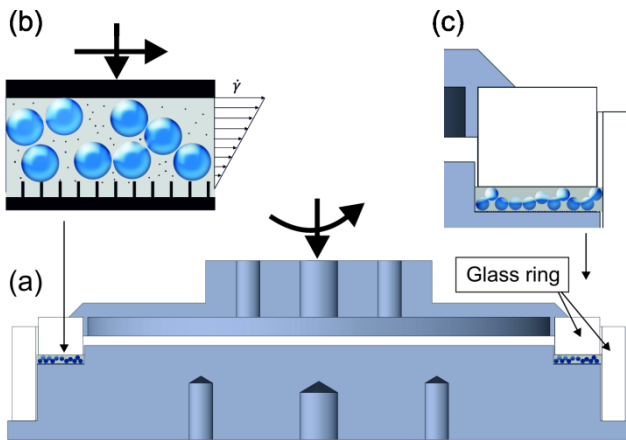


Figure 2: Schematic of the sample chamber.

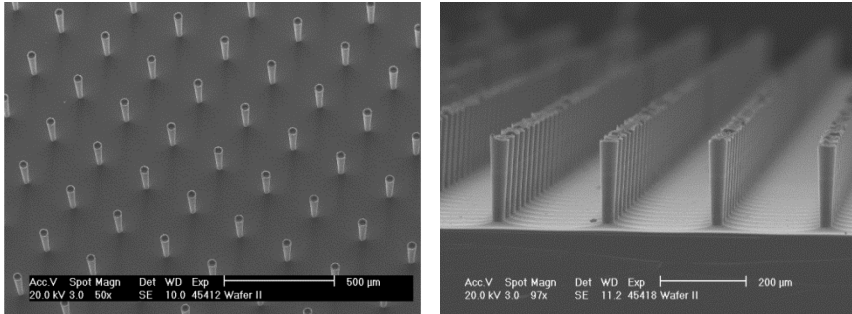


Figure 3: Scanning electron microscope image of a micro-pillar array.

studies using Particle-Image-Velocimetry (PIV), small fluorescent tracer particles in diameter  $20\ \mu\text{m}$  are added, too. The method of cross-correlation was applied to double-images in interrogation sizes of  $32 \times 32$  pixels with a Gaussian peak fitting procedure to detect the displacement vector with subpixel accuracy. The chip sensor size is  $1600 \times 1200$  px. The processing software is based on an inhouse matlab code which allows phase separation between solid and liquid phase. The uncertainty is of order of 0.1 pixel which equates to a velocity uncertainty of  $1 \times 10^{-5}$  m/s. Typical flow speeds are of order of  $10^{-3}$  m/s.

To study how the shape of particles' affects their motion, the slurry contained a few particles with two or three glued together. The volume concentration of the solid phase varied between 10% and 20%. The slurry layer thickness was varied in experiments and was adjusted typically to 2–3 diameters of the glass balls. The results of which are presented here were carried out at a shear rate  $\dot{\gamma} = 2\ \text{s}^{-1}$  and a slurry layer thickness of 1.5 mm. The slurry behaviour during shear loading was observed with CCD cameras from two sides of the flow chamber. Light emitting diodes provided illumination and filters ensured epifluorescent imaging. The liquid phase motion and its interaction with large particles were studied on the small-sized tracer-particles. Bending of the micro-pillars was detected by the reflections at the tip of the cantilever beams. Typical pictures of the flow as seen from top and from the side are given in Fig. 4.

### 3 Results and discussion

The optical access into the slurry gap allows the observation of particle behaviour in the suspension, the interaction between the liquid phase and particles, the movement of separate particles, their mutual interaction and the interaction with the micro-structured surface. From bending of the micro-pillars, we can estimate the contact forces by application of equations for a linear elastic Euler beam. The material constants such as Young-modulus of silicon are well described in literature. In addition, fracture of the structures is also a well defined event in the process since the position of fracture and the position of force is prescribed by the system (fracture happens at the micro-pillar foot, force is acting at the micro-pillar tip).

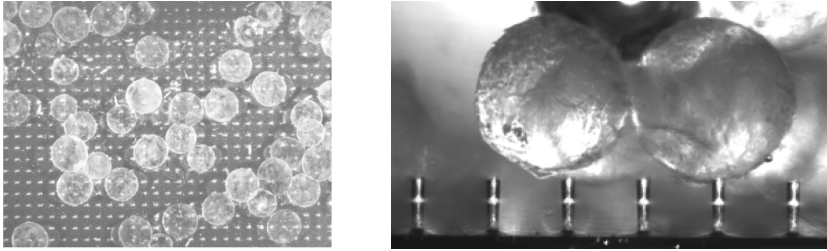


Figure 4: Pictures of the slurry in the shear cell. Left: top view on the slurry showing the reflections of the micro-pillars at the bottom wall as a regular grid (physical size of the image area is  $7 \times 5.5 \text{ mm}^2$ ). Right: side view demonstrating the micro-pillars and the glass balls above (physical size is  $1.5 \times 0.8 \text{ mm}^2$ ).

We have observed the following typical motion patterns which are described in the following, many of which can be seen on the photographs shown in Fig. 5. From a large sequence of images an excerpt of eight successive pictures is shown. In the pictures it is possible to watch the position of the numbered glass balls over the time. Furthermore, one can see the tips of the micro-pillars and some of them being broken and moving with the fluid. During shear loading of the slurry liquid phase, all particles (glass balls) in the solid phase start moving from the initial state.

Due to the velocity gradient, all particles come into rotation, too. Thanks to the uneven coating of the glass balls, we could not only determine the translational motion but also quantify particle rotation in the images. Moving speed and the rotation speed for particles being not in contact with other particles depends on their size and their position in the layer of a sheared suspension.

Translational speed of most of the particles coincides with the local velocity of the liquid phase. For example, the particles #39 (Fig. 5(f), 5(g)) and #28 (Fig. 5(e), 5(f)) which are moving in a layer of liquid closer to the rotating ring move faster in comparison to other particles. The speed of rotation relative to the translational speed of the particles increases when the particles came into contact with structured surfaces. In addition, the direction of movement of the liquid phase has impact on the path of the movement of single particles. As an example it is possible to watch the motion of particle #37 (Fig. 5(d), 5(e), 5(f)) and particle #44 (Fig. 5(g), 5(h)) with the liquid phase around a particle #38 which is slower than the others.

In Fig. 5 it is also demonstrated, that at a shear flow in a thin layer, many particles of the suspension, even at relatively low concentrations, cannot move independently. Due to the kinematic restrictions of the test chamber walls, their roughness (microstructures) affects strongly the behavior of particles. It is manifested by abrupt changes in the motion direction and the deceleration of translational and rotary motion of particles. In these cases, we observed a discrepancy between the velocities of the liquid layer and the particles. During contact with other particles, we watched them change their direction of rotation. The changes in rotation direction and the translational velocity of particle induce

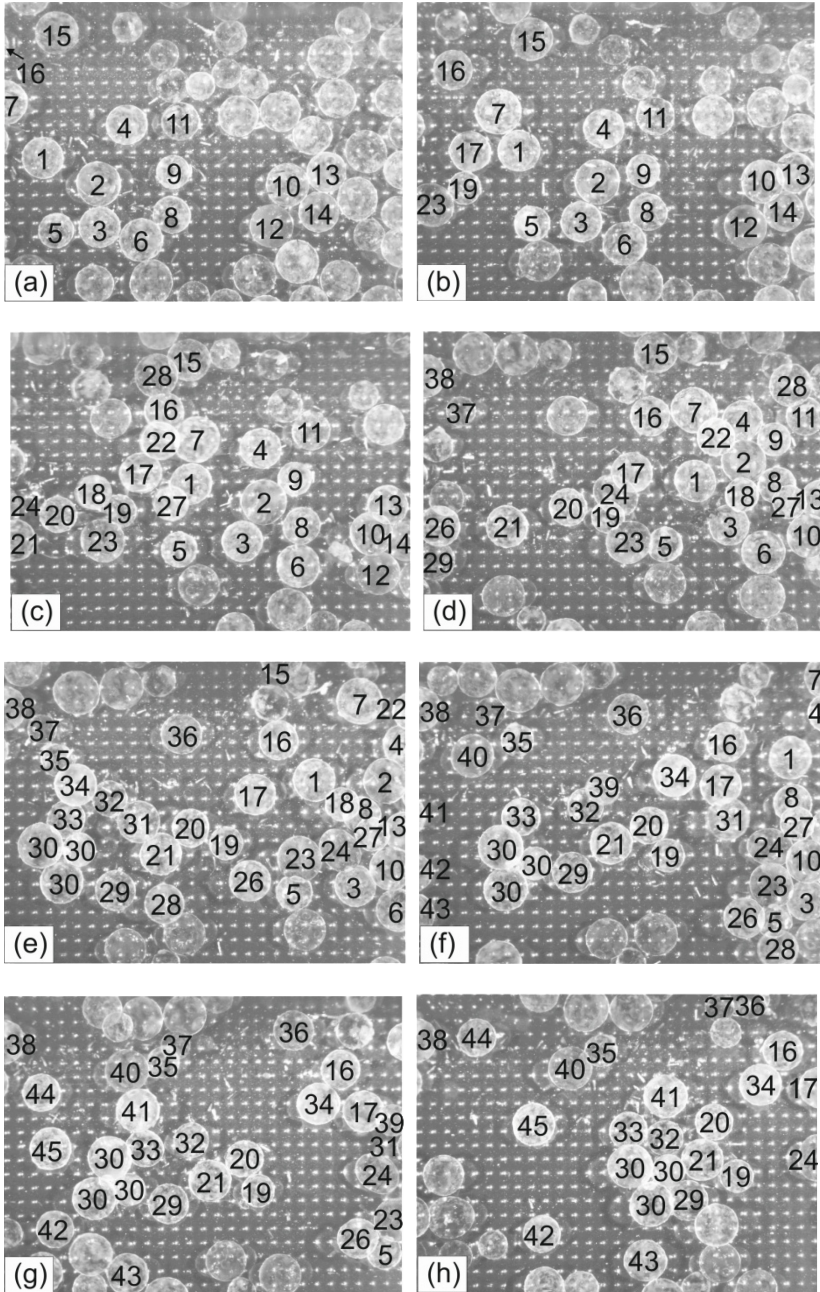


Figure 5: Image sequence showing the particle motion in the suspension under shear load of the slurry (flow is from left to right). The time step between successive images is about 1 second.

their mutual collisions and continuous formation and destruction of their aggregate structures of various types. The particles form differently oriented chains and compact structures of different density. These aggregate structures sometimes can remain for longer periods and continue to move as a unit. Moving chains sometimes are destroyed by individual particles which are in contact with the bottom wall.

The particles consisting of two or three glued balls (glued together) behave radically unlike from simple balls. The hydrodynamic forces that arise in a flow lead to orientation of an asymmetric particle relative to the streamlines. Because of the small thickness of a layer of sheared suspension rotation of such particles is partially limited. They decelerate typically more often and they tend to attach to the bottom wall and remain at rest. Their rotation is typically more complicated and periodical. In Figure 5(e), 5(f), 5(g), 5(h), we can observe the motion of a larger particle agglomerate (glued from three balls) as particle #30.

The interaction of particles with the bottom surface is indicated by the abrupt deceleration of movement and the tendency to stop. During the deformation of the suspension, many single particles contacted the structured surface of the chamber, but the event of a fracture of the micro-pillar could not be captured live in the sequence. However, from the flow of broken micro-pillars in the liquid phase we concluded that fracture events were appearing in a regular manner. As soon as a particle remains in contact with a micro-pillar and stops its motion, it prevents the free flow of other trailing particles and leads to structure's formation. Movement of particles #13 and #10 in Fig. 5 is an example of such behavior. After deceleration and coming to rest, subsequent movement of large particles or aggregates then causes high hydrodynamic drag forces and drastically enlarges the contact forces at the micro-pillar. This leads to the fracture of the micro-pillars in a defined manner (Fig. 6).

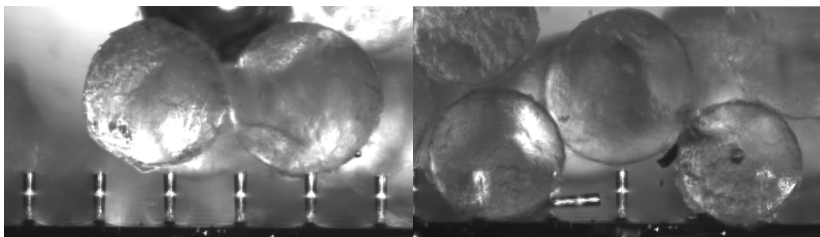


Figure 6: Interaction of particles with the micro-pillar surfaces.

Fig. 8 demonstrates the results of PIV-measurements in the suspension using the information of the fluorescent light scattered by the small tracer particles. It is obvious that path instabilities of the solid phase causes large disturbances in the flow of the liquid phase and therefore generates high fluctuations in the flow direction at different positions in the shear cell.

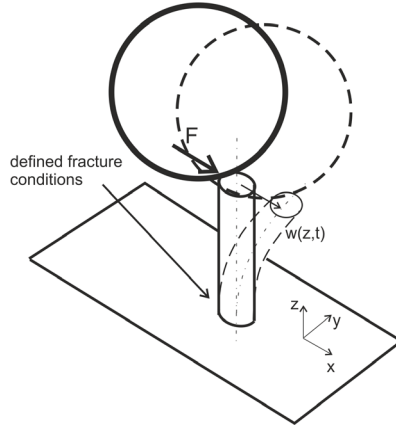


Figure 7: Principle of measuring the contact force by elastic bending of the micro-pillars. Note that critical load leads to well defined fracture of the structure at the foot which describes a well-defined mechanical condition and allows us to estimate maximum loads during shear deformation in the cell.

## 4 Conclusions

A new shear cell has been presented which allows the optical observation of cluster behaviour and contact forces in a suspension. The new mechanical model is well suited for comparison with theoretical studies due to the defined boundary conditions of micro-pillar bending and critical load when a fracture happens. Our visual observations showed that during rotation, contact and structure formation, the flow around the particles create largely different hydrodynamic forces which fluctuate in direction and magnitude. As a consequence flow patterns evolve which show micro-vortices resembling those that occur in locally turbulent flows. The largely fluctuating hydrodynamic drag forces also causes critical loads that lead to fracture of the micro-pillars. These events were documented by the broken micro-pillars that were flowing in the slurry after fracture. The design of the apparatus has a great influence on the test results. In the experimental studies carried out, the characteristic height of the shear cell was about 2–3 average particle diameters. In this case, the mechanical behavior of the suspension is not invariant with respect to the device, depending on its geometry and the roughness of the walls. In our device, the upper wall is allowed to adapt to the internal forces by axial motion against a spring. Therefore, there is volatility of the gap width as a consequence of material deformations in the direction orthogonal to the shear direction. Under such conditions, dilatancy can occur in the suspension. The latter can lead to the short appearance of larger suction pressures in the suspension.



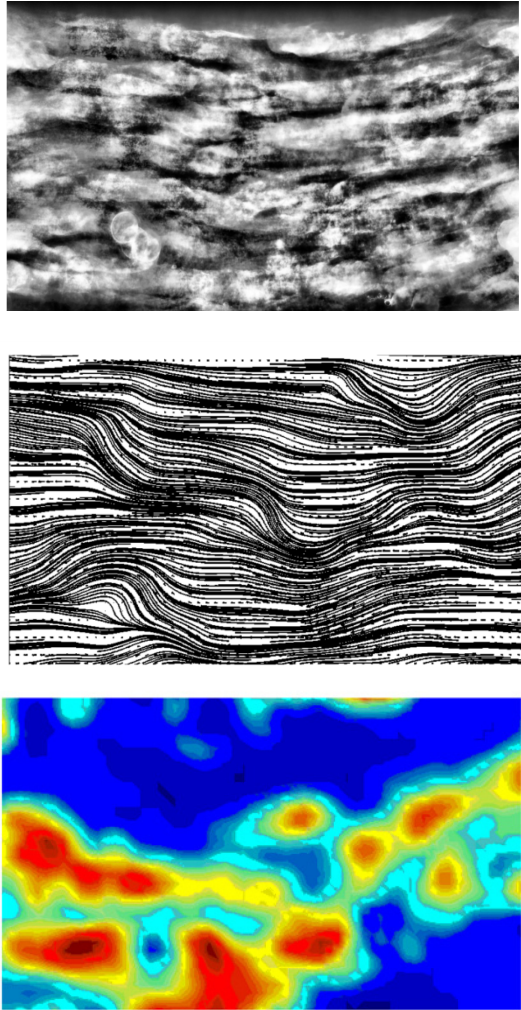


Figure 8: Representation of the particle and fluid motion statistics: Top: Average of image sequence showing preferred paths of particles and events of particle contacts with the bottom wall. Center: streamlines of the liquid phase showing regions of large disturbances where the flow is forced to swirl around clusters or particles at rest. Bottom: regions of high fluctuation energy of fluid motion (color bar from  $\langle u^2 \rangle / U^2 = 0.1$  in red to 0 in blue). Physical size of image area is  $11.6 \times 7 \text{ mm}^2$ .

## Acknowledgement

The Deutsche Forschungsgemeinschaft (DFG) supported the work under contract BR 1494/20-1.



## References

- [1] Bjerrum, L., and Landva, A., Direct simple shear tests on a Norwegian quick clay. *Geotechnique*, **16(1)**, pp. 1–20, 1966.
- [2] Bishop, A.W., Green G.E., Garga, V.K., Andresen, A., Brown J.D., A new ring-shear apparatus and its application to residual strength. *Geotechnique*, **21(4)**, pp. 273–328, 1971.
- [3] Bromhead, E. N., A Simple Ring Shear Apparatus. *Ground Engineering*, **12(5)**, pp. 40–44, 1979.
- [4] Carr, J.F. and Walker, D.M., An Annular Shear Cell for Granular Materials, *Powder Technology*, **1(6)**, pp. 369–373, 1968.
- [5] Brücker, Ch., Spatz, J., Schröder, W., Feasibility study of wall shear stress imaging using microstructured surfaces with flexible micropillars. *Exp. Fluids*, **39**, pp. 464–474, 2005.
- [6] Brücker, Ch., Signature of varicose wavepackets in the viscous sublayer. *Phys. Fluids*, **20**, 061701, 2008.

